

Phonon Frequency Spectrum and Lattice Dynamics and Normal Coordinate Analysis of HTSC $Tl_2Ca_2Ba_2Cu_3O_{10}$

K.Sonamuthu

J.N.R.Mahavidyalaya Port Blair, Andaman

Abstract

The lattice dynamics of the high temperature superconductors $Tl_2Ca_2Ba_2Cu_3O_{10}$ has been investigated on the basis of the three body force shell model (TSM). The various interactions between ions are treated on a general way without making them numerically equal. The phonon frequency at the zone centre of Brillouin zone are presented and the vibrational assignments are discussed. Further the normal coordinate calculation has also been employed to study the vibrational analysis of this compound. The normal coordinate analysis of the superconductor $Tl_2CaBa_2Cu_2O_8$ has been calculated by using Wilson's F-G matrix method which is useful for the confirmation of our present investigation. The vibrational frequencies and the potential energy distribution (PED) of the optically active phonon modes are also presented.

DOI: 10.7176/APTA/80-04

Publication date: October 31st 2019

1. Introduction

The study of the lattice dynamics of the high-temperature superconductors is of importance not only for the overall physical characterization of these compounds but also for an assessment of the role played by the phonons i.e., the superconducting phenomenon. A lattice dynamical study requires the knowledge of the crystal structure and the particle interactions. Usually the crystal structure is determined using X-ray diffraction. For particle interactions one has to use models, which represent the characteristic of the electronic structure and its effect on ionic interaction in a relevant manner. In lattice dynamics the ionic interactions are expressed in terms of force constants.

Cox et.al[1] have refined the structure of high-temperature superconductors $Tl_2Ca_2Ba_2Cu_3O_{10}$ using neutron and powder diffraction data. Raman and infrared active modes of $Tl_2Ca_2Ba_2Cu_3O_{10}$ have been calculated by Kulkarni et.al[2] in the frame work of shell models. Belosiudov et.al[3] have calculated vibrational spectrum of $Tl_2Ca_2Ba_2Cu_3O_{10}$ using interatomic interactions. A high resolution neutron diffraction study on $Tl_2Ca_2Ba_2Cu_3O_{10}$ is contributed by Ogborne et.al[4].

In the present work we start with a more general approach in the framework of the three body-force shell model (TSM) with $R \neq S \neq T$ to calculate the lattice dynamics frequencies. The values of the phonon frequencies calculated in this present work at zone center by the three body force shell model is in good agreement with the available Raman and infrared values. Further a normal coordinate analysis has also been attempted for the superconductor $Tl_2Ca_2Ba_2Cu_3O_{10}$ using Wilson's F-G matrix method for the confirmation of our present investigations. The vibrational frequencies and the potential energy distribution (PED) of the optically active modes are also reported.

2. Theoretical Consideration

2.1 Lattice dynamics of $Tl_2Ca_2Ba_2Cu_3O_{10}$ based on the shell model

The calculation of lattice dynamical vibration frequencies of $Tl_2Ca_2Ba_2Cu_3O_{10}$ system is performed by three-body force shell model (TSM) calculations. In the shell model calculation the equations of the motion for the core coordinate U and the shell coordinate W are expressed as follows:

$$\begin{aligned} -M\omega^2 U &= (R + ZC'Z) U + (T + ZC'Y) W \\ 0 &= (T' - YC'Z) U + (S + K + YC'Y) W \end{aligned}$$

With $ZC'Z = Z[Z + 2f(a)] C + V$ where M , Z and Y are diagonal matrices representing the mass ionic charge on the shell. R , S and T are matrices specifying short-range core-core, shell-shell and core-shell interactions, respectively. V is the matrix describing the three-body overlap interactions and $f(a)$ is related to overlap integrals of electron wave function. U and W are the vectors describing the ionic displacements and deformations respectively.

In the earlier approaches the R , S and T elements were considered to be equal to one another. In the present investigation, we have started with an approach such that $R \neq S \neq T$ [5]. That is the various interactions between the ions are treated in a more general way without making them numerically equal. The dynamical matrix of the model consists of long-range Coulomb and three-body interactions and the short-range overlap repulsions. The off-diagonal elements of this matrix along the symmetry directions chain a completely new term having a significant contribution for unequal R , S and T .

The lattice dynamical calculation of high-temperature superconductors is explained using an interionic potential consisting of long-range Coulomb part and a short-range Potential of Born-Mayer form [6]

$$V_{ij} = a_{ij} \exp(-b_{ij} r)$$

Where i, j label the ions and r is their separation. The parameters a_{ij} and b_{ij} are the pair potentials and the parameters Y and K determine the electronic polarizabilities. The parameters used in the present calculations are given in Table 1. Phonon frequencies are calculated using the force constants derived from the interionic potential. Following Leaner et al [7] interionic pair potentials for short-rang interactions can be transferred from one structure to another in similar environments. The force constants evaluated by this method are in good agreement with the evaluated values [8]

2.2 Normal coordinate analysis of the zero wave vector vibrations of $Tl_2Ca_2Ba_2Cu_3O_{10}$

The study of lattice vibrations and the free carriers is important for the understanding of the physical nature of high temperature superconductors. Raman and far-infrared studies of these superconductors have contributed significantly to the understanding of new class of superconductors. Cardona and coworkers [9] studied the infrared and Raman spectra of the super conducting cuprate perovskites $MBaCu_2O_2$ ($M = Nd, Er, Dy, Tm$ and Eu) and reproted the possible origins of phonon softening and the systematic variation of phonon frequencies with the ionic radius. Here an attempt has been made to perform the normal coordinate analysis for the phonon frequencies and the form of the zero wave vector vibrations for the $Tl_2Ca_2Ba_2Cu_3O_{10}$ superconductors.

The high T_c superconductor $Tl_2Ca_2Ba_2Cu_3O_{10}$ System crystallizes in the body-centered tetragonal (bct) system which belongs to the space group $14/mmm$ (D_{4h}^{17}). The body-centered tetragonal (bct) unit cell of $Tl_2Ca_2Ba_2Cu_3O_{10}$ and the numbering of the atoms are shown in Fig. 1. The 19 atoms of the unit cell yield a total of 38 optical vibrational modes. All of above calculations are made at $q = 0$. One of A_{2u} and E_u modes corresponds to acoustic vibrations with frequency

$\omega = 0$. These normal modes are distributed as follows.

$$\begin{aligned} A_{1g} + E_g + A_{2u} + E_u &\rightarrow \text{from the motion of 2Tl atoms} \\ A_{1g} + E_g + E_u &\rightarrow \text{from the motion of 2Ba atoms} \\ A_{1g} + E_g + A_{2u} + E_u &\rightarrow \text{from the motion of 2 Ca atoms} \\ A_{1g} + E_g + A_{2u} + E_u &\rightarrow \text{from the motion of 2 Cu(1) atoms} \\ A_{2u} + E_u &\rightarrow \text{from the motion of Cu(2) atoms} \\ A_{1g} + 2E_g + B_{1g} + 2A_{2u} + 2B_{2u} + 3E_u &\text{from the motion of O (1) atoms along c-axis.} \\ A_{1g} + E_{1g} + 2A_{2u} + 2E_u &\rightarrow \text{from the motion of O(2) atoms along the b-axis.} \\ A_{1g} + E_g + A_{2u} + E_u &\rightarrow \text{from the motion of O(3) atoms along the a-axis.} \end{aligned}$$

Subtracting the translation modes $A_{2u} + B_{2u} + E_u$ the $q = 0$ optical modes involved in an irreducible representation are as follows.

$$\Gamma_{opt} = 7 A_{1g} + B_{1g} + 8 E_g + 9 A_{2u} + 2 B_{2u} + 11 E_u$$

The species belonging to A_{1g} , B_{1g} and E_g are Raman active modes whereas A_{2u} and B_u are infrared active modes. The A_{2u} and A_{1g} modes involves displacement along crystallographic c-axis, the B_{2u} and E_g modes along the b-axis and the B_{1g} and E_u modes along the a-axis. The normal coordinate calculation was performed using the programs GMAT and FPERT given by Fuhrer et al [10]. The general agreement between the evaluated and observed normal frequencies of $Tl_2Ca_2Ba_2Cu_3O_{10}$ is good. The calculated force constants using the above programs are given in Table 2. It is interesting to note that the evaluated frequencies given in Table 3 agree favourably with the experimental values.

To check whether the chosen set of vibrational frequencies makes the maximum contribution to the potential energy associated with the normal coordinate frequencies of the superconducting material, the potential energy distribution was calculated using the equation.

$$PED = (F_{ij} L^2_{ik}) / \lambda_k$$

Where PED is the combination of the i -th symmetry coordinate to the potential energy of the vibration whose frequency is ν_k , F_{ij} are potential constants, L_{ik} , are L matrix elements and $\lambda_k = 4 \pi^2 C^2 \nu_k^2$.

3. Results and Discussion: ($Tl_2Ca_2Ba_2Cu_3O_{10}$)

3.1 Lattice Dynamical Calculations using Shell model.

The Lattice Dynamical Calculations based on modified TSM reproduce the observed frequencies of Raman and infrared active modes reasonable which are given in table 3. The calculated frequencies are in good agreement with the available experimental values. The lowest calculated active A_{1g} mode frequency at 104cm^{-1} is due to the vibration of Ba, Cu(1) and Cu(2) atoms and this agrees very well with the observed frequency at 99cm^{-1} . The evaluated Raman phonon frequency at 126cm^{-1} is due to the vibration of Tl, Ba and Cu(1) atoms and the observed frequency at 133cm^{-1} agrees very well with the calculated frequency. Here the Tl atom is vibrating 180° out of phase to Ba and Cu(1) atoms. Similarly thee calculated Raman phonon frequency at 144cm^{-1} is due to the vibration of Cu(1), Ba and Cu(2) atoms and Ba atom is vibrating 180° out of phase of Cu(1) and Cu(2) atoms and the observed frequency at 159cm^{-1} agrees very well with the calculated frequency. The next calculated Raman

phonon frequency at 290 cm^{-1} is due to the vibration of O(1), O(4) and Ca atoms and its observed frequency is 270 cm^{-1} . The evaluated Raman phonon frequency at 401 cm^{-1} is due to the vibration of O(1), O(4) and Ca atoms and the Ca atom is vibrating 180° out of phase to O (1) and O(4) atoms and the observed frequency 407 cm^{-1} agrees very well with the calculated frequency. The evaluated phonon frequency 489 cm^{-1} is due to Vibration of O(2) atoms. The maximum evaluated Raman frequency 608 cm^{-1} is due to the vibration of O(3) atoms and the observed frequency 601 cm^{-1} agrees very well with the calculated frequency. The evaluated Raman phonon frequency 256 cm^{-1} in B_{1g} Symmetry is due to the vibration of O(1) and O (4) atoms and the observed frequency 245 cm^{-1} agrees very well with calculated frequency.

Similarly, the evaluated Raman phonon frequency at 66 cm^{-1} in E_g symmetry is due to the vibration of Ba, Cu(1) atoms and are in plane with Ca atom. The Raman phonon frequency at 136 cm^{-1} is due to the vibration of Tl atom. The evaluated Raman frequency at 140 cm^{-1} is due to Cu(1), Ba and Ca atoms and Ba atom is vibrating 180° out of phase of Cu(1) and Ca atoms. The evaluated phonon frequency at 259 cm^{-1} is due to the bending vibration of O(1), O(4) and Ca atoms. The phonon frequency at 375 cm^{-1} due to stretching vibration of O(1) and O(4) atoms. The calculated phonon frequency 450 cm^{-1} is due to the vibration of O(2) atoms. The phonon frequency 489 cm^{-1} is due to the vibration of O(3) atom. The highest calculated phonon frequency at 555 cm^{-1} in E_g symmetry is due to the stretching vibration of O(1) atoms.

The lowest calculated infrared phonon frequency in A_{2u} symmetry at 72 cm^{-1} is due to the vibrations of $C_u(1)$ and $C_u(2)$ atoms and the observed frequency at 128 cm^{-1} agrees very well with the calculated frequency. The evaluated infrared phonon frequency at 103 cm^{-1} is due to the vibration of Cu(2), Cu(1) and Tl atoms in which Tl atom vibrates 180° out of phase to Cu(2) and Cu(1) atoms and the observed frequency 131 cm^{-1} agrees very well with the calculated frequency. The next evaluated infrared phonon frequency at 150 cm^{-1} is due to the vibration of Cu(2) and Cu(1) atoms and the observed frequency at 151 cm^{-1} agrees very well with the calculated frequency.

The evaluated infrared phonon frequency at 190 cm^{-1} is due to the vibration of O(4), O(1) and Ca atoms and its observed frequency 197 cm^{-1} agrees very well with the calculated phonon frequency. The next evaluated infrared phonon frequency at 365 cm^{-1} is due to the vibration of O(2), Ca and O(1) atoms. Here Ca atom is vibrating 180° out of phase to O(2) and O(1) atoms and the observed frequency at 372 cm^{-1} agrees very well with the calculated frequency. The calculated frequency at 420 cm^{-1} is due the vibration of O(4), O(2) and Ca atoms in which Ca atom vibrates 180° out of phase to O(4) and O(2) atoms and the observed frequency 421 cm^{-1} agrees very well with the calculated frequency. The next higher calculated infrared phonon frequency at 444 cm^{-1} is due to the vibration of O(2), O(1) and Ca atoms and the observed frequency at 454 cm^{-1} agrees very well with the calculated frequency. The highest calculated infrared phonon frequency in A_{2u} symmetry at 607 cm^{-1} is due to the vibration of O(3) atom and its observed frequency at 616 cm^{-1} agrees very well with the calculated frequency.

The evaluated phonon infrared frequency in B_{2u} symmetry at 133 cm^{-1} is due to the vibration of O(4) and O(1) atoms. The calculated frequency at 306 cm^{-1} is due to the vibration of O(4) and O(1) atoms.

The lowest calculated infrared phonon frequency in E_u symmetry is 70 cm^{-1} which is due to the vibration of Cu(2) and Tl atoms and the Tl atom is vibrating out of plane to Cu(2) atom and the observed frequency 70 cm^{-1} agrees very well with the calculated frequency. The calculated infrared frequency 101 cm^{-1} is due to the vibration of Tl and Cu(2) atoms and the observed frequency at 101 cm^{-1} agrees very well with the calculated phonon frequency. The evaluated infrared phonon frequency at 145 cm^{-1} is due to the vibration of Cu(1), Cu(2) and Ba atoms in which Ba atom is vibrating 180° out of phase to Cu(1) and Cu(2) atoms and the observed frequency at 145 cm^{-1} agrees very well with the calculated frequency. The calculated infrared frequency at 255 cm^{-1} is due to vibration of Cu O(4) and O(1) atoms which performs bending bond vibrations and the observed frequency at 255 cm^{-1} agrees very well with the calculated frequency. The next calculated infrared frequency at 359 cm^{-1} is due to the vibration of O(4) and O(1) atoms and the observed frequency at 359 cm^{-1} agrees very well with the calculated frequency. The calculated infrared phonon frequency at 387 cm^{-1} is due to the vibration of O(2) and O(3) atoms and the observed frequency at 397 cm^{-1} agrees very well with the calculated frequency.

The calculated infrared phonon frequency at 435 cm^{-1} is due to the vibration of Ca, O(1) and O(4) atoms. Here Ca atom vibrates 180° out of phase to O(1) and O(4) atoms and the observed frequency at 446 cm^{-1} agrees very well with the calculated frequency. The evaluated frequency at 451 cm^{-1} is due to the vibration of O(3) and O(2) atoms and the O(2) atom vibrates out of plane to O(3) atom and the observed frequency at 456 cm^{-1} agrees very well with the calculated frequency. The evaluated infrared frequency at 555 cm^{-1} is due to the vibration of O(1) atom which performs stretching vibrations and the observed frequency at 556 cm^{-1} agrees very well with the calculated frequency. The highest calculated infrared frequency in E_u symmetry at 569 cm^{-1} is due to the vibration of O(4) atom performs stretching vibration and the observed frequency 563 cm^{-1} agrees very well with the calculated frequency.

3.2 Normal coordinate analysis

The Normal Coordinate Analysis of $\text{Tl}_2\text{Ca}_2\text{Ba}_2\text{Cu}_3\text{O}_{10}$ reproduces the observed frequencies of Raman and infrared

active modes reasonable which are given in table 3. The calculated frequencies are in good agreement with the available experimental values. The lowest calculated active A_{1g} mode frequency at 110cm^{-1} is due to the vibration of Ba, Cu(1) and Cu(2) atoms. The evaluated Raman phonon frequency at 130cm^{-1} is due to the vibration of Tl, Ba and Cu(1) atoms. Here the Tl atom is vibrating 180° out of phase to Ba and Cu(1) atoms. Similarly the calculated Raman phonon frequency at 151cm^{-1} is due to the vibration of Cu(1), Ba and Cu(2) atoms and Ba atom is vibrating 180° out of phase of Cu(1) and Cu(2) atoms. The next calculated Raman phonon frequency at 281cm^{-1} is due to the vibration of O(1), O(4) and Ca atoms. The evaluated Raman phonon frequency at 412cm^{-1} is due to the vibration of O(1), O(4) and Ca atoms and the Ca atom is vibrating 180° out of phase to O(1) and O(4) atoms. The evaluated phonon frequency 486cm^{-1} is due to Vibration of O(2) atoms. The maximum evaluated Raman frequency 605cm^{-1} is due to the vibration of O(3) atoms. The evaluated Raman phonon frequency 261cm^{-1} in B_{1g} Symmetry is due to the vibration of O(1) and O(4) atoms.

Similarly, the evaluated Raman phonon frequency at 70cm^{-1} in E_g symmetry is due to the vibration of Ba, Cu(1) atoms and are in plane with Ca atom. The Raman phonon frequency at 142cm^{-1} is due to the vibration of Tl atom. The evaluated Raman frequency at 164cm^{-1} is due to Cu(1), Ba and Ca atoms and Ba atom is vibrating 180° out of phase of Cu(1) and Ca atoms. The evaluated phonon frequency at 270cm^{-1} is due to the bending vibration of O(1), O(4) and Ca atoms. The phonon frequency at 365cm^{-1} due to stretching vibration of O(1) and O(4) atoms. The calculated phonon frequency 411cm^{-1} is due to the vibration of O(2) atoms. The phonon frequency 471cm^{-1} is due to the vibration of O(3) atom. The highest calculated phonon frequency at 554cm^{-1} in E_g symmetry is due to the stretching vibration of O(1) atoms.

The lowest calculated infrared phonon frequency in A_{2u} symmetry at 81cm^{-1} is due to the vibrations of Cu(1) and Cu(2) atoms. The evaluated infrared phonon frequency at 120cm^{-1} is due to the vibration of Cu(2), Cu(1) and Tl atoms in which Tl atom vibrates 180° out of phase to Cu(2) and Cu(1) atoms. The next evaluated infrared phonon frequency at 148cm^{-1} is due to the vibration of Cu(2) and Cu(1) atoms. The evaluated infrared phonon frequency at 181cm^{-1} is due to the vibration of O(4), O(1) and Ca atoms. The next evaluated infrared phonon frequency at 369cm^{-1} is due to the vibration of O(2), Ca and O(1) atoms. Here Ca atom is vibrating 180° out of phase to O(2) and O(1) atoms. The calculated frequency at 411cm^{-1} is due the vibration of O(4), O(2) and Ca atoms in which Ca atom vibrates 180° out of phase to O(4) and O(2) atoms. The next higher calculated infrared phonon frequency at 449cm^{-1} is due to the vibration of O(2), O(1) and Ca atoms. The highest calculated infrared phonon frequency in A_{2u} symmetry at 592cm^{-1} is due to the vibration of O(3) atom.

The evaluated phonon infrared frequency in B_{2u} symmetry at 138cm^{-1} is due to the vibration of O(4) and O(1) atoms. The calculated frequency at 309cm^{-1} is due to the vibration of O(4) and O(1) atoms.

The lowest calculated infrared phonon frequency in E_u symmetry is 69cm^{-1} which is due to the vibration of Cu(2) and Tl atoms and the Tl atom is vibrating out of plane to Cu(2) atom. The calculated infrared frequency 105cm^{-1} is due to the vibration of Tl and Cu(2) atoms. The evaluated infrared phonon frequency at 152cm^{-1} is due to the vibration of Cu(1), Cu(2) and Ba atoms in which Ba atom is vibrating 180° out of phase to Cu(1) and Cu(2) atoms. The calculated infrared frequency at 228cm^{-1} is due to vibration of Cu O(4) and O(1) atoms which performs bending bond vibrations. The next calculated infrared frequency at 358cm^{-1} is due to the vibration of O(4) and O(1) atoms. The calculated infrared phonon frequency at 390cm^{-1} is due to the vibration of O(2) and O(3) atoms.

The calculated infrared phonon frequency at 441cm^{-1} is due to the vibration of Ca, O(1) and O(4) atoms. Here Ca atom vibrates 180° out of phase to O(1) and O(4) atoms. The evaluated frequency at 458cm^{-1} is due to the vibration of O(3) and O(2) atoms and the O(2) atom vibrates out of plane to O(3) atom. The evaluated infrared frequency at 562cm^{-1} is due to the vibration of O(1) atom which performs stretching vibrations. The highest calculated infrared frequency in E_u symmetry at 571cm^{-1} is due to the vibration of O(4) atom performs stretching vibration.

Vibrational modes on the region $400\text{-}500\text{cm}^{-1}$ are attributed to Ca-O(2) stretching. The present potential energy distribution confirms our conclusion. The lower frequency modes involve the small displacement of Ca-O(2) and Ba-O and the angular displacement of O-Ca-O. The evaluated frequencies using the normal coordinate analysis method listed in table 3 agree favourably with the calculated lattice dynamical frequencies and observed experimental frequencies.

4. Conclusion

The theoretical phonon frequencies obtained by the lattice dynamics and the normal coordinate analysis method agrees very well with the available Raman and infrared frequencies. This calculation attributes not only the phonon frequency in center of the Brillouin zone but also supports the strong electron-phonon interaction in the high-temperature superconductor $\text{Tl}_2\text{Ca}_2\text{Ba}_2\text{Cu}_3\text{O}_{10}$

References

- [1] D.E., Cox, C.C. TOVARADI, M.A., SUBRAMANIAN, J. GOPALKRISHNAN, and A.W. SLEIGHT, *Phys. Rev. B* **38**, 6624 (1988).
- [2] A.D. KULKARANI, J.PRADE, F.W. DE WATTE, W. KRESS, and U. SCHRODER, *Phys. Rev. B* **40**, 2624 (1989).
- [3] V.R. BELOSLUDOV, M.Y. LAVRENTIEV, and S.A. SYSKIN, *Int. J.Mod. Phys. B* **5**, 3109 (1991)
- [4] D.M. OGBORNE, M.T. WELLER, and P.C. LANCHESTER, *Physica C* **200**, 207 (1992)
- [5] S. MOHAN, S.DURAI, and G.VAIDYANATHAN, *Indian J.Phys.* **60A**, 137 (1986)
- [6] S. ONARI, T.HIROAKI, K.ONGHIME, H.HONME, and T. ARAI, *Solid State Commun.* **3**. 303 (1988)
- [7] N. LEHNER, H.RAUH, K.STROBEL, R.GEICK, G.HEGER, J. BOUILLOT, B.RENKER, M.ROUSSEAU, and W.J. STIRLING, *J. Phys. C* **15**, 6545 (1982).
- [8] S.ONARI, A.ONO, T.ARAI, and T.MORI, *Physica B* **165/166**, 1235 (1990).
- [9] C. THOMSEN, M.CARDONA, W.KRESS, L.GENZEL, M.BAUER, W.KING, and A.WITTLIN, *Soild State Commun.* **64**, 727 (1987)
- [10] H. FUHRER, V.B. KARTHA, K.G.KIDD, P.J. KRUEGER, and H.H. MANTASCH, *Computer Programs for Infrared Spectrometry, Vol. V, Normal Coordinate Analysis National Research Council of Canada, Ottawa 1976.*

Table :1

Parameters of the model: a, b are Born- Mayer constants: Z, Y, K, ionic charge, shell charge and on-site core-shell force constant of the ion, v_a is the volume of the unit cell

Interaction	a (eV)	b (\AA^{-1})
Tl-O (Same plane)	3000	2.80
Tl-O (adj plane)	3000	3.55
Ba-O	3220	2.90
Ca-O	2510	3.10
Cu-O	1260	3.35
O-O	1000	3.00

ion	Z(e)	Y(e)	$k(e^2 v_a)$
Tl	2.70	2.00	1000
Ba	2.00	2.32	207
Ca	2.02	-0.50	1350
Cu	2.00	3.22	1248
O(Cu-O) plane	-1.90	-2.70	310
O(Tl-O) plane	-1.93	-2.70	210
O(Ba-O) plane	-1.93	-2.70	310 ($K_{ }$) 2100(K_{\perp})

Table : 2

Force constants for $Tl_2Ca_2Ba_2Cu_3O_{10}$ (in units of 10^2 Nm^{-1} (stretching) and $10^{-18} \text{ Nm rad}^{-2}$ (bending))

Potential Constants	bond type	distance (\AA)	initial value
f_a	Ca-O(1)	2.467	1.06
f_b	Ba-O(1)	2.798	0.75
f_c	Ba-O(2)	2.819	1.10
f_d	Ba-O(3)	2.851	0.81
f_e	Tl-O(1)	2.003	0.30
f_g	Tl-O(2)	2.097	0.30
f_h	Tl-O(3)	3.108	0.61
f_k	Tl-O(3)	2.402	0.48
f_i	Cu-O(1)	1.932	0.145
f_m	Cu-O(2)	2.648	1.65
f_n	Tl-O(3) –Tl	--	0.31
f_p	O(1)-Cu-O(1)	--	0.25
f_a	Tl-O(2)-Ba	--	0.46
f_β	O(2)-Tl-O(3)	--	0.80

Table:3
Calculated Phonon frequencies of $Tl_2Ca_2Ba_2Cu_3O_{10}$ (Values in the Parentheses are experimental frequencies).

Symmetry species	Frequency(cm^{-1}) Using Lattice Dynamics	Using Normal Coordinate analysis	Potential Energy Distribution(%)	
A_{1g} (Raman)	104(99)	110	f_{β} (60) f_d (19) f_k (14)	
	126(133)	130	f_c (55) f_l (30)	
	144(159)	151	f_c (72) f_l (19)	
	290(270)	281	f_a (51) f_{α} (29)	
	401(407)	412	f_a (61) f_c (20) f_m (10)	
	489(498)	486	f_a (52) f_k (21) f_c (13)	
	608(601)	605	f_a (72) f_{α} (16)	
	B_{1g}	256(245)	261	f_a (56) f_k (14) f_{α} (10)
E_g		66	70	f_c (60) f_e (14) f_{β} (16)
	136	142	f_m (74) f_c (20)	
	140	164	f_c (41) f_m (20) f_l (19)	
	259	270	f_c (52) f_m (16) f_c (12)	
	375	365	f_a (42) f_g (33) f_n (16)	
	415	411	f_{β} (51) f_k (12) f_g (19)	
	489	471	f_n (65) f_h (20) f_m (17)	
	555	554	f_{α} (61) f_m (21)	
	A_{2u} (IR)	72(103)	81	f_n (70) f_{α} (24)
		128(131)	120	f_m (68) f_k (24) f_{α} (12)
150(151)		148	f_a (80) f_c (14)	
190(197)		181	f_a (74) f_c (20)	
365(372)		369	f_p (54) f_n (30)	
420(421)		411	f_p (62) f_{β} (18) f_n (10)	
444(454)		449	f_p (66) f_{β} (20) f_n (10)	
607(616)		592	f_{β} (40) f_{β} (19) f_n (11)	
B_{2u}	133	138	f_p (54) f_n (26) f_c (15)	
	306	309	f_a (40) f_g (35) f_n (10)	
E_u	70(70)	69	f_{β} (70) f_c (20)	
	101(101)	105	f_a (66) f_c (21)	
	145(145)	152	f_a (71) f_c (20)	
	225(225)	228	f_a (41) f_{α} (14) f_c (21)	
	359(359)	358	f_c (61) f_c (16) f_k (14)	
	387(397)	390	f_{β} (64), f_c	
	435(446)	441	f_{β} (56), f_g	
	451(456)	458	f_{β} (64) f_p (28)	
	555(556)	562	f_n (65) f_{α} (21)	
569(563)	571	f_{η} (71) f_{α} (20)		

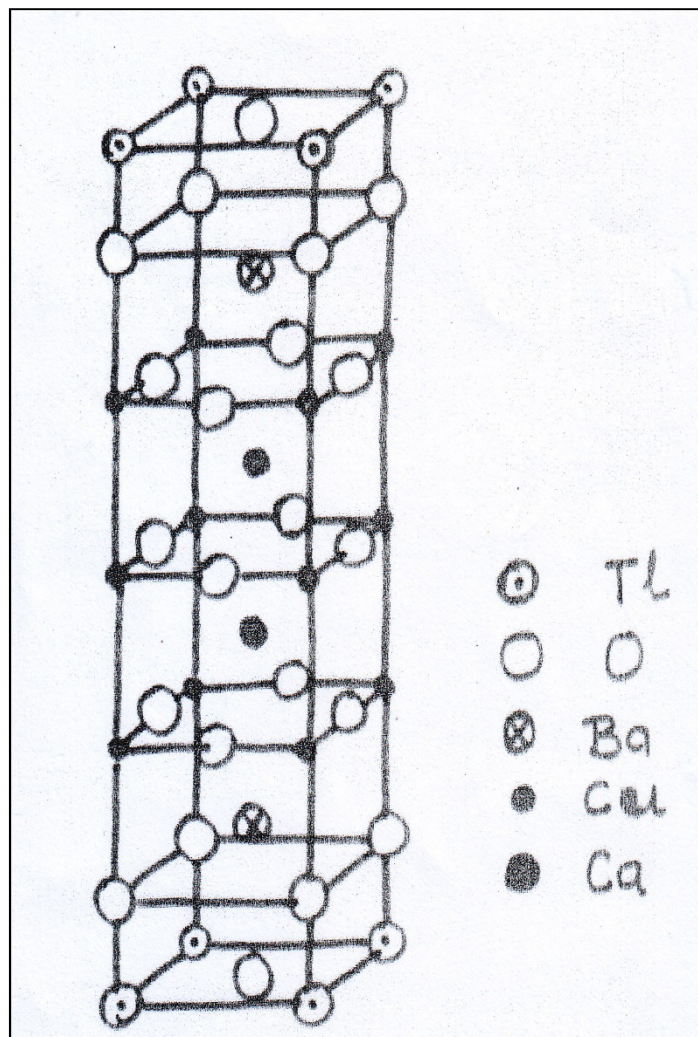


Fig. 1. Unit Cell of $Tl_2Ca_2Ba_2Cu_3O_{10}$